Synthesis and Chemistry of Icosahedral Bis(phosphine)metalladiarsaboranes and -distibaboranes Containing Nickel and Palladium. Crystal and Molecular Structures of *closo*-1,1-$(Me_2PPh)_2$-1,2,3-$PdAs_2B_9H_9$, *closo*-1,6-Cl_2-1,5-$(Me_2PPh)_2$-1,2,3-$PdAs_2B_9H_7 \cdot CH_2Cl_2$, and *closo*-1,1-$(Me_2PPh)_2$-1,2,3-$PdSb_2B_9H_9$

Steve A. Jasper, Jr., Steve Roach, John N. Stipp, J. C. Huffman, and Lee J. Todd*

Department of Chemistry and Molecular Structure Center, Indiana University, Bloomington, Indiana 47405

Received January 22, 1993

The reaction of $(Me_2PPh)_2MCl_2$ species (M = Ni or Pd) with the *nido*-7,8-$As_2B_9H_9^{2-}$ ion and $(Me_2PPh)_2PdCl_2$ with the *nido*-7,8-$Sb_2B_9H_9^{2-}$ ion at room temperature led to the formation of icosahedral bis(phosphine)metalladiheteroboranes in low to moderate yields for M = Ni(**1** for As) or M = Pd (**3** for As and **5** for Sb). In addition, *closo*-1-Cl-1,5-$(Me_2PPh)_2$-1,2,3-$NiAs_2B_9H_8$ (**2**) was isolated and fully characterized. In the palladium-containing reaction, the corresponding 6-chloro-substituted *closo*-1,6-Cl_2-1,5-$(Me_2PPh)_2$-1,2,3-$PdAs_2B_9H_7$ (**4**) was isolated. These complexes were formed by interchange of phosphine and hydrido ligands on the parent complex, followed by chlorine for hydrogen interchange. Compound **3** was characterized by an X-ray diffraction study. Purple crystals were monoclinic space group $P2_1/n$, with a = 12.874(3) Å, b = 10.421(3) Å, c = 19.555(6) Å, β = 104.08(1)°, and Z = 4. The structure was determined by conventional heavy-atom methods and refined to a final value of R = 0.0506 (3799 reflections), R_w = 0.0494. Compound **4** was characterized by an X-ray diffraction study. Green crystals were monoclinic space group $C2/c$, with a = 37.011(13) Å, b = 10.267(3) Å, c = 17.465(6) Å, β = 116.65(1)°, and Z = 8. The structure was determined by conventional heavy-atom methods and refined to a final value of R = 0.0780 (6080 reflections), R_w = 0.0731. Compound **5** was characterized by an X-ray diffraction study. Purple crystals were monoclinic space group $P2_1/n$, with a = 12.958(3) Å, b = 10.619(2) Å, c = 19.587(6) Å, β = 103.98(1)°, and Z = 4. The structure was determined by conventional heavy-atom methods and refined to a final value of R = 0.0301 (10158 reflections), R_w = 0.0338.

Introduction

We have previously reported an improved synthesis of 1,2-$As_2B_{10}H_{10}$ with $B_{10}H_{14}$, as the starting material.[1] Treatment of this icosahedral diarsaborane with excess piperidine forms the 7,8-$As_2B_9H_{10}^-$ ion in good yield.[2] This arsenic-containing monoanion which is isoelectronic with the well-known 7,8-$C_2B_9H_{12}^-$ ion may well form an extensive series of metal complexes similar to the well-known metallacarboranes.[3] In previous studies several metalladiarsaborane complexes such as $(C_5H_5)CoAs_2B_9H_9$, (dppe)$NiAs_2B_9H_9$ [dppe = 1,2-bis(diphenylphosphino)ethane], $L_2Pd(B_9H_9As_2)$, $L_2Pt(B_9H_9As_2)$, $LClPd(5\text{-}L\text{-}B_9H_8As_2)$ [L = PMe_2Ph or PPh_3], $(PPh_3)_2HRh(B_9H_9As_2)$, and $(C_5Me_5)Rh(B_9H_9As_2)$ have been reported.[1,4,5,6]

Substitution of a neutral ligand, such as a phosphine, for H^- on a B atom in a borane cage results in a "charge-compensated"[7] cage; that is, a cage formally one unit of charge more positive. In this specific case for arsaboranes, this corresponds to changing $B_9H_9As_2^{2-}$ to $B_9H_8(L)As_2^-$ (L = neutral 2 e^- donor).

Several metallaheteroborane complexes reported in the literature contain charge-compensating ligands. Methods of preparation include formal ligand rearrangement from the metal onto the cage,[8–10] reduction of a metallacarborane complex by a Lewis base,[11–13] addition of R_2S to a protonated metallocene-type sandwich complex,[14] and metalation of a charge-compensated carborane ligand.[7,15–18] In this report we describe the synthesis, chemistry, and X-ray structures of some new metalladiarsaborane complexes containing nickel and palladium and synthesis, chemistry, and an X-ray structure of a new metalladistibaborane complex containing palladium.

Experimental Section

Physical Measurements. Boron (^{11}B) NMR spectra were obtained at 115.85 MHz (21 °C) with a Nicolet NT-360 spectrometer and were externally referenced to $BF_3 \cdot OEt_2$. Phosphorus (^{31}P) NMR spectra were obtained at 146.2 MHz (21 °C) and externally referenced to 85% H_3PO_4. Proton (^1H) spectra were obtained at 361.1 MHz (21 °C) and internally referenced to $CHCl_3$. In all NMR spectra, positive chemical shifts were downfield. Infrared spectra were obtained as KBr pellets and recorded on either a Perkin-Elmer 283 spectrometer or a Nicolet 510P

(1) Hanusa, T. P.; Roig de Parisi, N.; Kester, J. G.; Arafat, A.; Todd, L. J. *Inorg. Chem.* **1987**, *26*, 4100.
(2) Little, J. L.; Pao, S. S.; Sugathan, K. K. *Inorg. Chem.* **1974**, *13*, 1752.
(3) Grimes, R. N. In *Organometallic Reactions and Syntheses*; Baker, E. I., Tsutsui, M., Eds.; Plenum Press: New York, 1977; Vol. 6, Chapter 2.
(4) Little, J. L.; Pao, S. S. *Inorg. Chem.* **1978**, *17*, 584.
(5) Fontaine, X. L. R.; Kennedy, J. D.; McGrath, M.; Spalding, T. R. *Magn. Reson. Chem.* **1991**, *29*, 711.
(6) McGrath, M.; Spalding, T. R.; Fontaine, X. L. R.; Kennedy, J. D.; Thornton-Pett, M. *J. Chem. Soc., Dalton Trans.* **1991**, 3223.
(7) Kang, H. C.; Lee, S. S.; Knobler, C. B.; Hawthorne, M. F. *Inorg. Chem.* **1991**, *30*, 2024.
(8) Miller, S. B.; Hawthorne, M. F. *J. Chem. Soc., Chem. Commun.* **1976**, 787.
(9) King, R. E., III; Miller, S. B.; Knobler, C. B.; Hawthorne, M. F. *Inorg. Chem.* **1983**, *22*, 3548.
(10) Greenwood, N. N.; Kennedy, J. D. *Pure Appl. Chem.* **1991**, *63*, 317.
(11) Jones, C. J.; Francis, J. N.; Hawthorne, M. F. *J. Am. Chem. Soc.* **1973**, *95*, 7633.
(12) Churchill, M. R.; Gold, K. *Inorg. Chem.* **1973**, *12*, 1157.
(13) Plesek, J.; Stibr, B.; Hermanek, S. *Czech. Chem. Commun.* **1984**, *49*, 1492.
(14) Hawthorne, M. F.; Warren, L. F., Jr.; Callahan, K. P.; Travers, N. F. *J. Am. Chem. Soc.* **1971**, *93*, 2407.
(15) Teller, R. G.; Wilczynski, J. J.; Hawthorne, M. F. *J. Chem. Soc. Chem. Commun.* **1979**, 472.
(16) Colquhoan, H. M.; Greenhough, T. J.; Wallbridge, M. G. H. *J. Chem. Soc., Dalton Trans.* **1979**, 619.
(17) Young, D. C.; Howe, D. V.; Hawthorne, M. F. *J. Am. Chem. Soc.* **1969**, *91*, 859.
(18) Kang, H. C.; Do, Y.; Knobler, C. B.; Hawthorne, M. F. *Inorg. Chem.* **1988**, *27*, 1716.

0020-1669/93/1332-3072$04.00/0

Fourier transform spectrometer. Ultraviolet–visible range spectra were recorded on a Hewlett-Packard 8452A diode array spectrophotometer. Melting points were obtained in sealed, evacuated capillaries and are uncorrected. Elemental analyses were performed by Schwarzkopf Microanalytical Laboratories, Woodside, NY.

Materials. All reactions were performed under an atmosphere of prepurified nitrogen. Tetrahydrofuran (THF) was freshly distilled from sodium benzophenone ketyl. Piperidine was distilled (106 °C) from sodium hydroxide prior to use. The arsaborane 1,2-$B_{10}H_{10}As_2$ was prepared by previous literature methods.[1] Similarly, the stibaborane 1,2-$B_{10}H_{10}Sb_2$ was prepared by previous literature methods.[19] Bis(dimethylphenylphosphine)nickel(II) chloride and bis(dimethylphenylphosphine)palladium(II) chloride were prepared by the method of Wild et al.[20] All other commercially available reagents were used as purchased.

1,1-(PMe_2Ph)$_2$-*closo*-1,2,3-$NiAs_2B_9H_9$ (1). In a two-neck round-bottom flask equipped with a septum and nitrogen inlet were placed 1,2-$B_{10}H_{10}As_2$ (270 mg, 1.01 mmol) and piperidine (5.0 mL, 51 mmol). The solid dissolved to form a light brown solution. After the mixture was stirred at room temperature for 2 h, the excess piperidine was removed *in vacuo*, to leave a gooey brown solid. Dry THF (50 mL) was added via syringe, followed by *n*-butyllithium (2.2 mmol = 2.2 equiv) in hexane solution, via syringe. The solution turned yellow immediately. Then, (PMe_2Ph)$_2NiCl_2$ (409 mg, 1.01 mmol) was added directly to the reaction mixture under N_2 purge. The mixture was stirred for 2 h, then the THF was removed under reduced pressure, and approximately 5 mL of CH_2Cl_2 and 2 g of silica gel (Merck grade 60, 130–270 mesh, 60 Å) was added. The solvents were removed under reduced pressure, and the solids were packed on a 40 cm × 2.4 cm silica gel chromatography column and eluted with 1:1 (v/v) toluene/CH_2Cl_2. There were two principal bands: band I was olive green, with R_f = 0.9 by TLC (CH_2Cl_2 mobile phase, Ag^+ development); band II was red, with R_f = 0.8. Recrystallization of band I from CH_2Cl_2/hexanes at 5 °C yielded small green crystals (161 mg, 27% yield). Mp: 172–175 °C dec. $^{11}B\{^1H\}$ NMR (CH_2Cl_2): δ 14.0, 6.1, 4.2, −7.2, and −8.9, in relative area ratio 1:3:2:2:1. $^{31}P\{^1H\}$ NMR (CH_2Cl_2): δ 0.6. ^1H NMR ($CDCl_3$): δ 1.568 (filled-in doublet, $^2J_{H-P}$ = 8.76 Hz), 7.40–7.45 (multiplets, arom), 7.61–7.69 (multiplets, arom). IR (in cm^{-1}): ν_{max} 3410 (w, br), 3210 (w, br), 3055 (w), 2960 (w), 2910 (w), 2570 (m), 2530 (vs), 2445 (m), 2365 (w), 2330 (w), 1433 (vs), 1315 (w), 1295 (w), 1285 (w), 1160 (w), 1098 (m), 999 (s), 945 (vs), 911 (vs), 745 (vs), 730 (m), 706 (vs), 695 (vs), 680 (m), 490 (m), and 426 (m). UV/vis spectrum (CH_2Cl_2): 450 (8.3 × 10^2 cm^{-1} M^{-1}) and 624 (64) nm. Anal. Calcd for $C_{16}H_{31}As_2B_9NiP_2$: C, 32.51; H, 5.28. Found: C, 31.94; H, 5.03.

1-Cl-1,5-(PMe_2Ph)$_2$-*closo*-1,2,3-$NiAs_2B_9H_8$ (2). Recrystallization of band II from CH_2Cl_2/hexanes at 5 °C yielded large, red, rectangular crystals (42 mg, 6% yield). Mp: 177–181 °C dec. $^{11}B\{^1H\}$ NMR (CH_2Cl_2): δ 9.2(doublet, J_{B-P} = 130 Hz), 1.6(singlet), 0.7(singlet), −4.4(singlet), and −8.5(singlet), in relative area ratio 1:2:2:1:3. $^{31}P\{^1H\}$ NMR ($CDCl_3$): δ −6.0(singlet), −4.7(1:1:1:1 quartet, J_{P-B} = 131 Hz). ^1H NMR ($CDCl_3$): δ 1.478(doublet, $^2J_{H-P}$ = 10.48 Hz), 1.940(doublet, $^2J_{H-P}$ = 12.12 Hz), 7.36–7.40 (multiplets, arom), 7.52–7.62 (multiplets, arom), and 7.69–7.75 (multiplets, arom). IR (in cm^{-1}): ν_{max} 3210 (w, br), 3070 (w), 2980 (w), 2920 (w), 2550 (vs), 2530 (vs), 2510 (vs), 2370 (w), 2340 (w), 1500 (w), 1430 (s), 1410 (m), 1320 (m), 1110 (m), 1100 (m), 1070 (w), 1020 (m), 980 (m), 960 (m), 940 (vs), 910 (vs), 860 (m), 760 (m), 740 (s), 710 (m), 690 (s), 680 (m), 480 (s), and 420 (m). Anal. Calcd for $C_{16}H_{30}As_2B_9ClNiP_2$: C, 30.72; H, 4.83. Found: C, 30.68; H, 4.75.

1,1-(PMe_2Ph)$_2$-*closo*-1,2,3-$PdAs_2B_9H_9$ (3). In a two-neck round-bottom flask equipped with a septum and nitrogen inlet were placed 1,2-$B_{10}H_{10}As_2$ (802 mg, 2.99 mmol) and piperidine (5.0 mL, 51 mmol). The solid dissolved to form a light brown solution. After the mixture was stirred at room temperature for 2 h, the excess piperidine was removed *in vacuo*, to leave a gooey brown solid. Dry THF (50 mL) was added via syringe, followed by *n*-butyllithium (6.8 mmol = 2.3 equiv) in hexanes solution, via syringe. The solution turned yellow immediately. After the mixture was stirred for 20 min, $PdCl_2(PMe_2Ph)_2$ (1.358 g, 2.994 mmol) was added directly to the reaction mixture under N_2 purge. The solution immediately turned dark brown. After 45 min, the THF was removed *in vacuo*, and approximately 5 mL of 1:1 (v/v) toluene/CH_2Cl_2 and 2 g of silica gel (60 Å, 230–400 mesh) were added. The solvents were removed *in vacuo*, and the solids were packed on a 40 cm × 2.2 cm silica gel chromatography column, and eluted with 1:1 toluene/CH_2Cl_2. There were two principal bands: band I was purple, with R_f = 0.8 by TLC (CH_2Cl_2 mobile phase); band II was green, with R_f = 0.2. The solvent was stripped off, and the solids were kept under a N_2 atmosphere. Several recrystallizations of band I from 1:1 hexanes/CH_2Cl_2 at 5 °C yielded large, purple, rectangular crystals (1.091 g, 57% yield). Mp: 143–145 °C dec. ^{11}B NMR (acetone): δ 11.4 (J_{B-H} = 130 Hz), 5.2 (136), 4.1 (130), −6.9 (151), and −11.9 (145), in 3:2:1:1:2 area ratio. $^{31}P\{^1H\}$ NMR (CH_2Cl_2): δ −3.4. ^1H NMR ($CDCl_3$): δ 1.605 (filled-in doublet, J_{H-P} = 9.01 Hz), 7.35–7.55 (br multiplet, arom). IR (in cm^{-1}): ν_{max} 2950 (w), 2880 (w), 2510 (vs), 2340 (m), 1470 (w), 1430 (s), 1400 (m, br), 1290 (w), 1270 (w), 1100 (m), 1060 (w), 990 (s), 940 (s), 905 (vs), 895 (vs), 830 (w), 740 (s), 720 (m), 700 (s), 680 (s), 480 (m), and 410 (m). UV/vis spectrum (CH_2Cl_2): 334 (ε = 1.3 × 10^4 cm^{-1} M^{-1}), and 538 (1.0 × 10^2) nm.

1,6-Cl_2-1,5-(PMe_2Ph)$_2$-1,2,3-$PdAs_2B_9H_7$ (4). In a two-neck round-bottom flask equipped with a septum and nitrogen inlet were placed (PMe_2Ph)$_2$Pd($B_9H_9As_2$) (400 mg, 0.626 mmol), (PMe_2Ph)$_2PdCl_2$ (285 mg, 0.628 mmol), 40 mL of dry CH_2Cl_2, and 20 mL of dry THF. The mixture was stirred for 12 days, and then the solvents were removed *in vacuo*. Dichloromethane was added until all solids were in solution (approximately 5 mL), and approximately 2 g of silica gel (60Å, 230–400 mesh) was added. The solvents were then removed *in vacuo*, and the silica gel containing the compounds was placed at the top of a 40 cm × 2.4 cm chromatography column, already packed with fresh silica gel. Elution with 1:1 (v/v) toluene/CH_2Cl_2 revealed three principal bands. Band I (R_f = 0.9 by TLC with CH_2Cl_2 mobile phase, development in Ag^+) was determined to be unreacted starting material, (PMe_2Ph)$_2$Pd($B_9H_9As_2$), and was recovered in 24% yield. Band III, the most polar (R_f = 0.5), was the previously reported[6] (PMe_2Ph)ClPd(5-$PMe_2PhB_9H_8$-As_2). It was recrystallized to yield 79 mg (19%). Band II was olive green, with R_f = 0.7. The solvents were stripped off to yield 73 mg (17%) of a semicrystalline material. $^{11}B\{^1H\}$ NMR (CH_2Cl_2): δ 10.4, 3.0 (doublet, J_{B-P} = 130 Hz), −0.9, −3.1, −7.7, −9.5, −11.7, and −15.6 in area ratio 2:1:1:1:1:1:1:1. $^{31}P\{^1H\}$ NMR (CH_2Cl_2): δ −1.2, −2.9 (1:1:1:1 quartet, J_{P-B} = 137 Hz). ^1H NMR ($CDCl_3$): δ 1.900 (doublet, $^2J_{H-P}$ = 12.70 Hz), 2.034 (doublet, $^2J_{H-P}$ = 10.59), 2.062 (doublet, $^2J_{H-P}$ = 10.62), 2.094 (doublet, $^2J_{H-P}$ = 12.46), 7.45–7.55 (multiplet, arom), 7.59–7.66 (multiplet, arom), and 7.80–7.87 (multiplet, arom).

1,1-(PMe_2Ph)$_2$-*closo*-1,2,3-$PdSb_2B_9H_9$ (5). In a two-neck round-bottom flask equipped with a septum and nitrogen inlet were placed 1,2-$B_{10}H_{10}Sb_2$ (1000 mg, 2.765 mmol) and piperidine (5.0 mL, 51 mmol). The solid dissolved, resulting in a dark green-brown solution. After the mixture was stirred at room temperature for 2 h, the excess piperidine was removed *in vacuo*, to leave a brown solid. Dry THF (40 mL) was added via syringe, followed by *n*-BuLi (6.12 mmol = 2.2 equiv) in hexanes solution, via syringe. After this mixture was stirred for 10 min, $PdCl_2(PMe_2Ph)_2$ (1255 mg, 2.767 mmol) was added directly to the reaction mixture under N_2 purge. The solution immediately turned deep purple. After 2 h, the THF was removed *in vacuo*, and approximately 5 mL of CH_2Cl_2 and 2 g of silica gel (60 Å, 230–400 mesh) were added. The CH_2Cl_2 was removed *in vacuo*, and the solids were packed on a 40 cm × 3.0 cm silica gel chromatography column, and eluted with 1:1 (v/v) toluene/CH_2Cl_2. The major fraction was grape purple, with R_f = 0.9 by TLC (CH_2Cl_2 mobile phase, Ag^+ development). The solvent was stripped off, and the solids kept under a N_2 atmosphere. Several recrystallizations from CH_2Cl_2/hexane at 5 °C yielded small rodlike purple crystals (514 mg, 25% yield). Mp: 208–211 °C dec. ^{11}B NMR (CH_2Cl_2): δ 20.8 (J_{B-H} = 130 Hz), 5.8 (142), 3.3 (138), 0.6 (123), −9.5, in 1:1:2:2:3 area ratio. $^{31}P\{^1H\}$ NMR ($CDCl_3$): δ −12.4. ^1H NMR ($CDCl_3$): δ 1.539 (filled-in doublet, J_{H-P} = 8.61 Hz), 7.36–7.48 (multiplets, arom). IR (in cm^{-1}): ν_{max} 3050 (w), 3007 (w), 2965 (w), 2905 (w), 2500 (vs, br), 1960 (w), 1889 (w), 1815 (w), 1570 (w), 1487 (w), 1476 (w), 1433 (s), 1416 (s), 1325 (w), 1310 (w), 1296 (w), 1281 (m), 1181 (w), 1157 (w), 1101 (m), 1073 (w), 1026 (w), 995 (s, br), 947 (s), 905 (s), 841 (m), 745 (s), 735 (s), 710 (s), 694 (s), 677 (m), 488 (s), 440 (w), and 424 (m).

Crystal Structure Determinations. The diffractometer utilized for data collection was designed and constructed locally. A Picker four-circle goniostat equipped with a Furnas monochromator (HOG crystal) and Picker X-ray generator was interfaced to a Z80 microprocessor which was controlled by an RS232 serial port on an IBM PC microcomputer. Motors were slo-syn stepping motors, and a special top/bottom–left/right slit assembly was used to align each crystal. All computations were performed on IBM compatible microcomputer systems using DOS or OS/2 operating systems.

(19) Little, J. L. *Inorg. Chem.* **1979**, *18*, 1598.
(20) Roberts, N. K.; Skelton, B. W.; White, A. H.; Wild, S. B. *J. Chem. Soc., Dalton Trans.* **1982**, 2093.

Table I. Selected Bond Distances (Å) for 1,1-$(PMe_2Ph)_2$-1,2,3-$PdAs_2B_9H_9$ (**3**)

	(i) to the Pd		
Pd(1)–As(2)	2.6835(18)	Pd(1)–B(4)	2.298(11)
Pd(1)–As(3)	2.5304(13)	Pd(1)–B(5)	2.283(12)
Pd(1)–P(1)	2.3108(27)	Pd(1)–B(6)	2.309(10)
Pd(1)–P(2)	2.3272(26)		
	(ii) to As		
As(2)–As(3)	2.4885(15)	As(3)–B(4)	2.259(12)
As(2)–B(6)	2.184(11)	As(3)–B(7)	2.235(11)
As(2)–B(7)	2.215(12)	As(3)–B(8)	2.119(12)
As(2)–B(11)	2.127(11)		
	(iii) Interboron		
B(4)–B(5)	1.755(16)	B(7)–B(11)	1.835(15)
B(4)–B(8)	1.859(16)	B(7)–B(12)	1.765(17)
B(4)–B(9)	1.773(15)	B(8)–B(9)	1.775(16)
B(5)–B(6)	1.881(17)	B(8)–B(12)	1.779(15)
B(5)–B(9)	1.774(16)	B(9)–B(10)	1.740(16)
B(5)–B(10)	1.785(16)	B(9)–B(12)	1.774(17)
B(6)–B(10)	1.819(16)	B(10)–B(11)	1.805(17)
B(6)–B(11)	1.872(15)	B(10)–B(12)	1.782(16)
B(7)–B(8)	1.871(17)	B(11)–B(12)	1.782(16)

Table II. Selected Bond Angles (deg) for 1,1-$(PMe_2Ph)_2$-1,2,3-$PdAs_2B_9H_9$ (**3**)

As(2)–Pd(1)–As(3)	56.93(4)	Pd(1)–P(1)–C(14)	113.9(4)
As(2)–Pd(1)–B(6)	51.2(3)	Pd(1)–P(1)–C(15)	121.6(4)
As(3)–Pd(1)–B(4)	55.5(3)	Pd(1)–P(1)–C(16)	111.5(3)
B(4)–Pd(1)–B(5)	45.0(4)	Pd(1)–P(2)–C(23)	117.1(4)
B(5)–Pd(1)–B(6)	48.4(4)	Pd(1)–P(2)–C(24)	108.9(4)
P(1)–Pd(1)–P(2)	97.56(9)	Pd(1)–P(2)–C(25)	118.8(3)
Pd(1)–As(2)–As(3)	58.44(4)	Pd(1)–As(3)–As(2)	64.64(4)
Pd(1)–As(2)–B(6)	55.50(28)	Pd(1)–As(3)–B(4)	57.01(27)
As(3)–As(2)–B(7)	56.4(3)	As(2)–As(3)–B(7)	55.6(3)
B(6)–As(2)–B(11)	51.5(4)	B(4)–As(3)–B(8)	50.1(4)
B(7)–As(2)–B(11)	49.9(4)	B(7)–As(3)–B(8)	50.8(4)
As(3)–As(2)–B(6)	94.2(3)	B(8)–B(7)–B(11)	104.8(8)
As(2)–As(3)–B(4)	98.8(3)	B(7)–B(8)–B(9)	108.3(8)
As(3)–B(4)–B(5)	116.0(8)	B(8)–B(9)–B(10)	109.0(9)
B(4)–B(5)–B(6)	110.8(8)	B(9)–B(10)–B(11)	110.0(8)
As(2)–B(6)–B(5)	120.0(7)	B(7)–B(11)–B(10)	107.6(8)

For **3** and **5**, data were collected using a moving crystal–moving detector technique with fixed background counts at each extreme of the scan (see Tables III and IX for complete unit cell parameters). A purple crystal of $(PMe_2Ph)_2Pd(B_9H_9As_2)$ (**3**) with dimensions 0.25 × 0.25 × 0.25 mm was transferred to the goniostat where it was cooled to −171 °C for characterization and data collection. A purple crystal of $(PMe_2Ph)_2Pd(B_9H_9Sb_2)$ (**5**) with dimensions 0.162 × 0.190 × 0.350 mm was transferred to the goniostat where it was cooled to −173 °C for characterization and data collection. A systematic search of a limited hemisphere of reciprocal space revealed a set of diffraction maxima with symmetry and systematic absences corresponding to the unique monoclinic space group $P2_1/n$. Subsequent solution and refinement confirmed this choice. Data were corrected for Lorentz, polarization, and absorption effects and averaged to yield a set of unique intensities. The structures were readily solved by direct methods phasing (MULTAN78) and Fourier techniques. All hydrogen atoms were clearly visible in difference Fouriers phased on the non-hydrogen atoms. In the final cycles of refinement, hydrogen atoms were assigned isotropic thermal parameters and non-hydrogen atoms anisotropic thermal parameters. The final difference Fouriers were featureless, the largest peak being 0.56 e/Å^3 for **3**, and the largest peaks for **5** (less than 0.8 e/Å^3) were in the vicinity of the Sb atoms.

For 1,6-Cl_2-1,5-$(PMe_2Ph)_2$-*closo*-1,2,3-$PdAs_2B_9H_7{\cdot}CH_2Cl_2$ (**4**), data were collected using a continuous theta, 2θ scan technique with fixed backgrounds at each extreme of the scan. (See Table VI for complete unit cell parameters.) A small green plate of **4** with dimensions 0.04 × 0.12 × 0.16 mm was transferred to the goniostat where it was cooled to −154 °C for characterization and data collection. A systematic search of a limited hemisphere of reciprocal space located a set of diffraction maxima with monoclinic symmetry and systematic absences corresponding to a *C*-centered space group with a *C* glide indicating space groups $C2/c$ or Cc. Subsequent solution and refinement of the structure confirmed the centrosymmetric choice, $C2/c$. Due to the small size of the crystal, only about one-third of the data were observed using the normal 2.33σ criteria. In spite of this, the structure was readily solved by direct methods (MULTAN78) and standard Fourier techniques. Because of the scarcity of data, only the palladium, arsenic, chlorine, and phosphorus atoms were assigned anisotropic thermal parameters during the refinement. All of the hydrogen atoms associated with the boron cage were visible in a difference Fourier phased on the non-hydrogen atoms, and they and the remaining hydrogens were thus placed in fixed positions for the final

Table III. Crystallographic Data for 1,1-$(PMe_2Ph)_2$-1,2,3-$PdAs_2B_9H_9$ (**3**)

mol wt = 638.90	scan speed = 8.0°/min
cryst system: monoclinic, $P2_1/n$, $Z = 4$	scan width = 2.0° + dispersion
unit cell	single bkgd time at extremes of scan = 4 s
a = 12.874(3) Å	aperture size = 3.0 × 4.0 mm
b = 10.421(3) Å	collection limit (2θ) = 6–45°
c = 19.555(6) Å	tot. no. of reflcns: 3799
β = 104.08(1)°	no. of unique intens: 3315
V = 2544.74 Å^3	no. with $F > 0.0$: 3045
ρ_{calcd} = 1.668 g cm^{-3}	no. with $F > 2.33*\sigma(F)$: 2715
λ = 0.710 69 Å	R for averaging: 0.020
μ = 34.243 cm^{-1}	final residuals
detector–sample dist = 22.5 cm	$R(F)$ = 0.0506
sample–source dist = 23.5 cm	$R_w(F)$ = 0.0494
take off angle = 2.0°	GOF for last cycle = 1.174
av ω scan width at half-height = 0.25°	max Δ/σ for last cycle = 0.05

Table IV. Selected Bond Distances (Å) for 1,6-Cl_2-1,5-$(PMe_2Ph)_2$-1,2,3-$PdAs_2B_9H_7{\cdot}CH_2Cl_2$ (**4**)

	(i) to the Pd		
Pd(1)–As(2)	2.445(5)	Pd(1)–B(4)	2.28(4)
Pd(1)–As(3)	2.684(5)	Pd(1)–B(5)	2.24(4)
Pd(1)–Cl(13)	2.386(9)	Pd(1)–B(6)	2.23(4)
Pd(1)–P(14)	2.305(10)		
	(ii) to As		
As(2)–As(3)	2.517(5)	As(3)–B(4)	2.17(4)
As(2)–B(6)	2.26(4)	As(3)–B(7)	2.21(5)
As(2)–B(7)	2.26(5)	As(3)–B(8)	2.11(5)
As(2)–B(11)	2.14(5)		
	(iii) Interboron		
B(4)–B(5)	1.85(5)	B(7)–B(11)	1.85(6)
B(4)–B(8)	1.92(7)	B(7)–B(12)	1.81(6)
B(4)–B(9)	1.86(6)	B(8)–B(9)	1.78(6)
B(5)–B(6)	1.73(5)	B(8)–B(12)	1.88(6)
B(5)–B(9)	1.79(5)	B(9)–B(10)	1.74(5)
B(5)–B(10)	1.77(6)	B(9)–B(12)	1.77(5)
B(6)–B(10)	1.82(6)	B(10)–B(11)	1.80(6)
B(6)–B(11)	1.91(6)	B(10)–B(12)	1.77(6)
B(7)–B(8)	1.87(6)	B(11)–B(12)	1.65(6)
	(iv) Other		
B(5)–P(24)	1.95(3)	P(14)–C(17)	1.83(4)
B(6)–Cl(23)	1.81(4)	P(24)–C(25)	1.82(4)
P(14)–C(15)	1.78(3)	P(24)–C(26)	1.81(4)
P(14)–C(16)	1.84(4)	P(24)–C(27)	1.82(3)

Table V. Selected Bond Angles (deg) for 1,6-Cl_2-1,5-$(PMe_2Ph)_2$-1,2,3-$PdAs_2B_9H_7{\cdot}CH_2Cl_2$ (**4**)

As(2)–Pd(1)–As(3)	58.56(14)	Pd(1)–P(14)–C(15)	119.2(13)
As(2)–Pd(1)–B(6)	57.5(11)	Pd(1)–P(14)–C(16)	111.2(12)
As(3)–Pd(1)–B(4)	50.9(10)	Pd(1)–P(14)–C(17)	112.5(13)
B(4)–Pd(1)–B(5)	48.4(13)		
B(5)–Pd(1)–B(6)	45.6(13)		
Cl(13)–Pd(1)–P(14)	85.8(3)		
Pd(1)–As(2)–As(3)	65.46(14)	Pd(1)–As(3)–As(2)	55.98(13)
Pd(1)–As(2)–B(6)	56.5(11)	Pd(1)–As(3)–B(4)	54.9(11)
As(3)–As(2)–B(7)	54.6(11)	As(2)–As(3)–B(7)	56.8(11)
B(6)–As(2)–B(11)	51.5(16)	B(4)–As(3)–B(8)	53.3(17)
B(7)–As(2)–B(11)	49.5(16)	B(7)–As(3)–B(8)	51.3(17)
As(3)–As(2)–B(6)	99.0(10)	B(8)–B(7)–B(11)	103.(3)
As(2)–As(3)–B(4)	93.4(10)	B(7)–B(8)–B(9)	106.(3)
As(3)–B(4)–B(5)	119.6(22)	B(8)–B(9)–B(10)	115.(3)
B(4)–B(5)–B(6)	113.7(26)	B(9)–B(10)–B(11)	103.(3)
As(2)–B(6)–B(5)	114.0(24)	B(7)–B(11)–B(10)	113.(3)

Table VI. Crystallographic Data for 1,6-Cl_2-1,5-$(PMe_2Ph)_2$-*closo*-1,2,3-$PdAs_2B_9H_7$·CH_2Cl_2 (**4**)

mol wt = 792.72	scan speed = 6.0°/min
crystal syst: monoclinic, $C2/c$, $Z = 8$	scan width = 2.0° + dispersion
unit cell	single bkgd time at extremes of scan = 3 s
$a = 37.011(13)$ Å	aperture size = 3.0 × 4.0 mm
$b = 10.267(3)$ Å	collcn limit (2θ) = 6–45°
$c = 17.465(6)$ Å	tot. no. of reflcns: 6080
$\beta = 116.65(1)°$	no. of unique intens: 3851
$V = 5931.81$ Å^3	no. with $F > 0.0$: 3019
$\rho_{calcd} = 1.775$ g cm^{-3}	no. with $F > 2.33*\sigma(F)$: 1393
$\lambda = 0.710\ 69$ Å	R for averaging: 0.077
$\mu = 33.092$ cm^{-1}	final residuals
detector–sample dist = 22.5 cm	$R(F) = 0.0780$
sample–source dist = 23.5 cm	$R_w(F) = 0.0731$
take off angle = 2.0°	GOF for last cycle = 1.101
av ω scan width at half-height = 0.25°	max Δ/σ for last cycle = 0.09

Table VII. Selected Bond Distances for 1,1-$(PMe_2Ph)_2$-1,2,3-$PdSb_2B_9H_9$ (**5**)

	(i) to the Pd		
Pd(1)–Sb(2)	2.7865(7)	Pd(1)–B(4)	2.290(4)
Pd(1)–Sb(3)	2.7074(8)	Pd(1)–B(5)	2.304(4)
Pd(1)–P(13)	2.3391(10)	Pd(1)-B(6)	2.290(4)
Pd(1)–P(22)	2.3287(12)		
	(ii) to Sb		
Sb(2)–Sb(3)	2.7996(7)	Sb(3)–B(4)	2.448(4)
Sb(2)–B(6)	2.393(4)	Sb(3)–B(7)	2.450(4)
Sb(2)–B(7)	2.472(4)	Sb(3)–B(8)	2.310(4)
Sb(2)–B(11)	2.306(4)		
	(iii) Interboron		
B(4)–B(5)	1.779(5)	B(7)–B(11)	1.831(6)
B(4)–B(8)	1.888(5)	B(7)–B(12)	1.753(6)
B(4)–B(9)	1.781(5)	B(8)–B(9)	1.795(6)
B(5)–B(6)	1.828(6)	B(8)–B(12)	1.780(5)
B(5)–B(9)	1.784(6)	B(9)–B(10)	1.754(6)
B(5)–B(10)	1.781(6)	B(9)–B(12)	1.776(6)
B(6)–B(10)	1.784(5)	B(10)–B(11)	1.788(6)
B(6)–B(11)	1.889(6)	B(10)–B(12)	1.770(6)
B(7)–B(8)	1.849(6)	B(11)–B(12)	1.771(6)
	(iv) other		
P(13)–C(14)	1.830(4)	P(22)–C(23)	1.819(4)
P(13)–C(15)	1.822(4)	P(22)–C(24)	1.820(4)
P(13)–C(16)	1.828(3)	P(22)–C(25)	1.816(4)

cycles of refinement. A final difference Fourier was essentially featureless, the largest peak being 0.34 e/Å^3. In spite of the small crystal, the structure is well resolved although the esd's associated with the distances and angles are somewhat excessive for a low-temperature study.

Results and Discussion

Reaction of *nido*-7,8-$As_2B_9H_{10}^-$ with *n*-butyllithium and then $(PMe_2Ph)_2MCl_2$ (M = Ni, Pd, or Pt) afforded the corresponding bis(phosphine)metalladiarsaborane complexes in low to moderate yield, eq 1. The Pd and Pt complexes have been reported elsewhere.[6] In the reaction with the nickel reagent one other compound in addition to **1** was formed in low yield. This second compound (**2**) is believed to be formed by a phosphine–hydrogen interchange to give $(PMe_2Ph)HNi(5\text{-}PMe_2Ph\text{-}B_9H_8As_2)$ which then undergoes hydrogen–chlorine exchange to generate **2**. The numbering system for these icosahedral metallaheteroboranes is as illustrated in Figure 1. In the reaction with the palladium reagent, the same phosphine–hydride interchange is observed to occur with $(PMe_2Ph)_2Pd(B_9H_9As_2)$, which has been reported.[6] However, under suitable conditions, the palladium complex can be further converted to a 6-chloro substituted complex (**4**) as well.

Table VIII. Selected Bond Angles (deg) for 1,1-$(PMe_2Ph)_2$-1,2,3-$PdSb_2B_9H_9$ (**5**)

P(13)–Pd(1)–P(22)	96.81(4)	Pd(1)–P(13)–C(14)	122.17(13)
Sb(2)–Pd(1)–Sb(3)	61.253(18)	Pd(1)–P(13)–C(15)	113.36(13)
Sb(2)–Pd(1)–B(6)	55.19(10)	Pd(1)–P(13)–C(16)	111.69(11)
Sb(3)–Pd(1)–B(4)	57.95(10)	Pd(1)–P(22)–C(23)	110.12(14)
B(4)–Pd(1)–B(5)	45.56(13)	Pd(1)–P(22)–C(24)	119.82(13)
B(5)–Pd(1)–B(6)	46.89(14)	Pd(1)–P(22)–C(25)	116.20(12)
Pd(1)–Sb(2)–Sb(3)	57.980(19)	Pd(1)–Sb(3)–Sb(2)	60.767(15)
Pd(1)–Sb(2)–B(6)	51.81(9)	Pd(1)–Sb(3)–B(4)	52.46(9)
Sb(3)–Sb(2)–B(7)	54.97(9)	Sb(2)–Sb(3)–B(7)	55.71(10)
B(6)–Sb(2)–B(11)	47.38(15)	B(4)–Sb(3)–B(8)	46.64(13)
B(7)–Sb(2)–B(11)	44.90(15)	B(7)–Sb(3)–B(8)	45.60(14)
Sb(3)–Sb(2)–B(6)	90.62(9)	B(8)–B(7)–B(11)	104.7(3)
Sb(2)–Sb(3)–B(4)	92.94(9)	B(7)–B(8)–B(9)	108.64(27)
Sb(3)–B(4)–B(5)	121.55(23)	B(8)–B(9)–B(10)	108.1(3)
B(4)–B(5)–B(6)	109.80(26)	B(9)–B(10)–B(11)	109.7(3)
Sb(2)–B(6)–B(5)	124.85(22)	B(7)–B(11)–B(10)	108.46(28)

Table IX. Crystallographic Data for 1,1-$(PMe_2Ph)_2$-1,2,3-$PdSb_2B_9H_9$ (**5**)

mol wt = 732.56	scan speed = 6.0°/min
cryst syst: monoclinic, $P2_1/n$, $Z = 4$	scan width = 2.0° + dispersion
unit cell	single bkgd time at extremes of scan = 6 s
$a = 12.958(3)$ Å	aperture size = 3.0 × 4.0 mm
$b = 10.619(3)$ Å	collcn limit (2θ) = 6–65°
$c = 19.587(6)$ Å	total no. of reflcns: 10158
$\beta = 103.98(1)°$	no. of unique intensities: 9457
$V = 2615.40$ Å^3	no. with $F > 0.0$: 8823
$\rho_{calcd} = 1.860$ g cm^{-3}	no. with $F > 3.00*\sigma(F)$ 6995
$\lambda = 0.710\ 69$ Å	R for averaging 0.020
$\mu = 28.627$ cm^{-1}	final residuals
detector–sample dist = 22.5 cm	$R(F) = 0.0301$
sample–source dist = 23.5 cm	$R_w(F) = 0.0338$
take off angle = 2.0°	GOF for last cycle = 1.000
av ω scan width at half-height = 0.25°	max Δ/σ for last cycle = 0.01

nido-7,8-$As_2B_9H_{10}^-$ + *n*-BuLi + $(PMe_2Ph)_2MCl_2$ →

closo-1,1-$(PMe_2Ph)_2$-1,2,3-$MAs_2B_9H_9$ + *n*-BuH + LiCl + Cl^- (1)

M = Ni (1), Pd (3), or Pt

Reaction of *nido*-7,8-$Sb_2B_9H_{10}^-$ with *n*-butyllithium and then $(PMe_2Ph)_2PdCl_2$ has so far yielded only the corresponding bis(phosphine)metalladistibaborane complex (**5**) in low yield, eq 2.

nido-7,8-$Sb_2B_9H_{10}^-$ + *n*-BuLi + $(PMe_2Ph)_2PdCl_2$ →

closo-1,1-$(PMe_2Ph)_2$-1,2,3-$PdSb_2B_9H_9$ + *n*-BuH + LiCl + Cl^- (2)

The C_s symmetry of the 1,2,3-$NiAs_2B_9H_9$ icosahedral configuration expected for **1** leads to a predicted 2:2:2:1:1:1 peak area ratio in the ^{11}B NMR spectrum. The actual ^{11}B NMR spectrum has a 1:3:2:2:1 peak area ratio due to unresolved overlap of an area 1 and area 2 peak. The single ^{31}P resonance in **1** suggests that at 21 °C there is rapid rotation of the metal vertex in the icosahedral structure relative to the pentagonal bonding face of the diarsaborane ligand.

^1H NMR. In the ^1H NMR spectra of the bis(phosphine) analogues $(PMe_2Ph)_2M(B_9H_9X_2)$, where M = Ni, Pd, or Pt and X = As or Sb, the *P*-methyl region of the spectrum exhibits an unusual three-line signal, perhaps best described as a doublet with a broad singlet overlapping it. This "motif" is consistently present in all analogues so far observed and so is not a case of accidentally overlapping peaks. Also, variable temperature NMR

Table X. Fractional Coordinates and Isotropic Thermal Parameters for 1,1-$(PMe_2Ph)_2$-1,2,3-$PdAs_2B_9H_9$ (3)[a]

atom	x	y	z	B_{iso},[b] Å^2
Pd(1)	4601(1)	704(1)	2327.7(4)	11
As(2)	2951(1)	−696(1)	1598.4(5)	16
As(3)	2724(1)	884(1)	2505.3(5)	14
B(4)	3604(9)	2557(12)	2174(6)	15
B(5)	4223(10)	2262(12)	1483(6)	19
B(6)	3913(9)	595(11)	1123(5)	13
B(7)	1693(9)	802(12)	1407(6)	17
B(8)	2137(9)	2408(12)	1799(6)	17
B(9)	2990(10)	3106(11)	1312(6)	16
B(10)	3206(9)	2000(12)	694(6)	18
B(11)	2435(9)	565(12)	726(6)	16
B(12)	1921(9)	2097(12)	881(5)	16
P(13)	6084(2)	−297(3)	2101(1)	15
C(14)	6681(9)	571(11)	1478(6)	19
C(15)	7263(9)	−628(12)	2796(6)	21
C(16)	5755(7)	−1903(10)	1730(5)	17
C(17)	5808(8)	−2225(11)	1055(5)	17
C(18)	5511(8)	−3442(10)	792(5)	17
C(19)	5182(8)	−4335(11)	1197(5)	19
C(20)	5105(8)	−4031(10)	1876(6)	19
C(21)	5409(8)	−2820(10)	2134(5)	18
P(22)	5296(2)	1056(3)	3527(1)	14
C(23)	4343(10)	1407(13)	4055(6)	22
C(24)	6141(10)	2464(12)	3640(7)	25
C(25)	6099(7)	−204(9)	4055(5)	12
C(26)	5717(8)	−1441(12)	3995(5)	20
C(27)	6304(9)	−2471(11)	4346(5)	20
C(28)	7301(9)	−2218(12)	4773(5)	22
C(29)	7667(9)	−979(12)	4861(6)	22
C(30)	7088(8)	41(11)	4515(5)	16
H(1)	377(6)	324(8)	255(4)	5(7)
H(2)	493(7)	276(8)	136(4)	14(5)
H(3)	429(6)	3(8)	78(4)	7(5)
H(4)	77(7)	30(8)	129(4)	13(3)
H(5)	146(6)	293(8)	192(4)	6(5)
H(6)	299(7)	408(9)	119(5)	21(4)
H(7)	333(7)	228(8)	20(5)	15(5)
H(8)	216(6)	−3(7)	22(4)	5(6)
H(9)	123(6)	250(7)	47(4)	6(7)
H(10)	719(8)	24(9)	141(5)	14(3)
H(11)	611(8)	71(9)	110(5)	19(4)
H(12)	694(6)	132(8)	175(4)	8(4)
H(13)	727(6)	−139(8)	312(4)	6(5)
H(14)	788(7)	−99(8)	267(4)	5(7)
H(15)	758(6)	15(9)	304(4)	7(5)
H(16)	596(6)	−162(8)	77(4)	4(7)
H(17)	561(7)	−360(8)	35(5)	11(4)
H(18)	491(7)	−507(9)	105(4)	8(5)
H(19)	491(9)	−465(12)	214(6)	41(3)
H(20)	537(6)	−252(8)	254(5)	8(5)
H(21)	477(8)	171(10)	446(6)	24(3)
H(22)	412(7)	218(9)	395(4)	6(5)
H(23)	391(9)	72(11)	406(6)	29(3)
H(24)	626(6)	277(8)	406(5)	5(4)
H(25)	676(7)	232(8)	350(4)	8(5)
H(26)	575(7)	314(9)	350(5)	9(5)
H(27)	522(7)	−165(9)	387(5)	3(5)
H(28)	612(7)	−325(9)	432(4)	5(5)
H(29)	769(7)	−287(8)	502(4)	6(5)
H(30)	815(7)	−81(9)	506(5)	3(3)
H(31)	735(7)	78(8)	456(4)	3(7)

[a] Fractional coordinates are ×10^4 for non-hydrogen atoms and ×10^3 for hydrogen atoms. B_{iso} values are ×10. [b] Isotropic values for those atoms refined anisotropically are calculated using the formula given by: Hamilton, W. C. *Acta Crystallogr.* **1959**, *12*, 609.

studies (+50 to −50 °C) on the Pd and Pt analogues indicate that the spectrum does not change with temperature, which suggests that this is not a stereochemical nonrigidity phenomenon. Rather, we believe this to be a case of partial virtual coupling of the two P atoms. With normal $^2J_{H-P}$ coupling, one expects a doublet due to splitting by one $I = {}^1/_2$ P atom, with perhaps small splitting of each peak from the other P ($^2J_{P-P} \ll {}^2J_{H-P}$). As the P–M–P angle approaches 180°, however, $^2J_{P-P} \gg {}^2J_{H-P}$, and the two P nuclei behave as though they are magnetically equivalent in

Table XI. Fractional Coordinates and Isotropic Thermal Parameters for 1,6-Cl_2-1,5-$(PMe_2Ph)_2$-1,2,3-$PdAs_2B_9H_7$-CH_2Cl_2 (4)[a]

atom	x	y	z	B_{iso},[b,c] Å^2
Pd(1)	4099(1)	1964(3)	557(2)	15
As(2)	4659(1)	496(4)	1387(2)	20
As(3)	4172(1)	851(4)	2010(2)	22
B(4)	3645(12)	708(42)	777(25)	18(7)
B(5)	3710(10)	297(36)	−189(21)	5(7)
B(6)	4211(12)	133(43)	10(27)	22(8)
B(7)	4369(13)	−1096(46)	1818(28)	28(8)
B(8)	3819(14)	−826(53)	1474(31)	36(9)
B(9)	3576(11)	−975(38)	336(23)	12(7)
B(10)	3899(13)	−1299(46)	−122(28)	29(9)
B(11)	4390(13)	−1307(46)	788(28)	28(8)
B(12)	4008(11)	−1968(45)	892(25)	18(7)
Cl(13)	3659(2)	3771(8)	346(6)	19
P(14)	4534(3)	3458(9)	429(6)	17
C(15)	5028(9)	2951(36)	626(20)	20(6)
C(16)	4630(11)	4832(37)	1174(22)	26(7)
C(17)	4336(12)	4144(42)	−651(25)	34(8)
C(18)	4071(9)	5229(34)	−863(20)	14(6)
C(19)	3929(10)	5716(38)	−1671(22)	25(7)
C(20)	4019(11)	5242(40)	−2289(24)	31(8)
C(21)	4274(10)	4205(39)	−2072(22)	26(7)
C(22)	4425(10)	3665(35)	−1253(22)	20(7)
Cl(23)	4409(3)	265(9)	−762(6)	20
P(24)	3279(3)	723(10)	−1321(6)	20
C(25)	3233(10)	−595(37)	−2059(22)	26(7)
C(26)	3393(11)	2211(39)	−1726(24)	31(8)
C(27)	2791(9)	912(33)	−1311(19)	11(6)
C(28)	2525(11)	−85(38)	−1525(23)	29(7)
C(29)	2140(11)	149(38)	−1520(23)	26(7)
C(30)	2044(11)	1222(38)	−1291(24)	29(7)
C(31)	2317(11)	2259(37)	−1116(23)	26(7)
C(32)	2691(10)	2151(34)	−1131(21)	19(7)
Cl(33)	2330(3)	6133(11)	9242(6)	33
C(34)	2843(10)	5946(37)	9490(22)	25(7)
Cl(35)	2937(3)	6056(11)	8614(7)	36
H(1)	336*	129*	71*	30
H(2)	456*	−174*	242*	30
H(3)	463*	−205*	79*	30
H(4)	379*	−198*	−73*	30
H(5)	326*	−145*	2*	30
H(6)	365*	−125*	186*	30
H(7)	401*	−311*	94*	30
H(8)	517*	271*	121*	30
H(9)	501*	223*	27*	30
H(10)	516*	365*	50*	30
H(11)	479*	454*	174*	30
H(12)	477*	549*	104*	30
H(13)	438*	516*	111*	30
H(14)	400*	561*	−45*	30
H(15)	375*	645*	−181*	30
H(16)	391*	561*	−285*	30
H(17)	435*	384*	−248*	30
H(18)	460*	293*	−112*	30
H(19)	317*	−138*	−186*	30
H(20)	302*	−40*	−261*	30
H(21)	348*	−69*	−209*	30
H(22)	364*	211*	−176*	30
H(23)	318*	240*	−228*	30
H(24)	342*	291*	−135*	30
H(25)	259*	−92*	−168*	30
H(26)	195*	−54*	−170*	30
H(27)	180*	132*	−125*	30
H(28)	225*	308*	−97*	30
H(29)	286*	288*	−103*	30
H(30)	299*	662*	989*	30
H(31)	293*	512*	975*	30

[a] Fractional coordinates are ×10^4 for non-hydrogen atoms and ×10^3 for hydrogen atoms. B_{iso} values are ×10. [b] Isotropic values for those atoms refined anisotropically are calculated using the formula given by: Hamilton, W. C. *Acta Crystallogr.* **1959**, *12*, 609. [c] Parameters marked by an asterisk were not varied.

splitting the methyl protons, so one expects a 1:2:1 triplet—i.e., the P nuclei are said to be virtually coupled.[21] In the present case of $(PMe_2Ph)_2Pd(B_9H_9As_2)$ and $(PMe_2Ph)_2Pd(B_9H_9Sb_2)$, the P–Pd–P angles are 97.56(9) and 96.81(4)°, respectively, so one

Table XII. Fractional Coordinates and Isotropic Thermal Parameters for 1,1-$(PMe_2Ph)_2$-1,2,3-$PdSb_2B_9H_9$ (**5**)[a]

atom	x	y	z	B_{iso},[b] Å^2
Pd(1)	335.4(3)	720.2(4)	7669.4(2)	10
Sb(2)	1883.1(3)	-916.1(3)	8416.3(2)	14
Sb(3)	2297.0(3)	763.7(3)	7413.2(2)	12
B(4)	1357(5)	2500(6)	7827(3)	14
B(5)	691(5)	2281(5)	8512(3)	15
B(6)	930(5)	682(6)	8872(3)	16
B(7)	3234(5)	771(6)	8669(3)	18
B(8)	2833(5)	2326(6)	8245(3)	13
B(9)	1943(5)	3056(6)	8696(3)	18
B(10)	1674(5)	1981(6)	9306(3)	18
B(11)	2403(5)	574(6)	9293(3)	17
B(12)	2963(5)	2056(6)	9158(3)	17
P(13)	-1144(1)	-354(1)	7861(1)	14
C(14)	-2297(4)	-713(6)	7143(3)	21
C(15)	-1789(5)	464(6)	8461(3)	20
C(16)	-789(4)	-1923(5)	8234(3)	14
C(17)	-510(4)	-2844(5)	7805(3)	17
C(18)	-192(4)	-4011(6)	8069(3)	21
C(19)	-161(4)	-4306(5)	8767(3)	20
C(20)	-432(4)	-3385(5)	9196(3)	18
C(21)	-751(4)	-2206(5)	8926(3)	15
P(22)	-380(1)	1190(1)	6488(1)	14
C(23)	-1320(5)	2485(6)	6408(4)	21
C(24)	486(5)	1746(7)	5946(3)	21
C(25)	-1092(4)	-71(5)	5950(3)	14
C(26)	-2086(4)	85(6)	5486(3)	18
C(27)	-2608(5)	-936(6)	5133(3)	22
C(28)	-2184(5)	-2117(6)	5228(3)	22
C(29)	-1173(5)	-2291(6)	5665(3)	20
C(30)	-642(5)	-1277(5)	6014(3)	18
H(1)	42(4)	17(5)	915(3)	20(7)
H(2)	-1(4)	277(4)	854(2)	7(7)
H(3)	103(5)	321(6)	738(3)	45(7)
H(4)	399(6)	43(7)	869(4)	51(7)
H(5)	264(5)	8(6)	972(3)	37(7)
H(6)	149(5)	226(6)	983(3)	36(7)
H(7)	201(5)	411(6)	876(3)	38(7)
H(8)	-258(5)	10(6)	691(3)	27(8)
H(9)	-214(5)	-126(6)	679(3)	32(8)
H(10)	-277(5)	-103(6)	731(3)	34(7)
H(11)	-122(6)	74(6)	890(4)	49(6)
H(12)	-210(5)	122(7)	825(4)	42(8)
H(13)	-232(5)	-11(6)	851(3)	31(7)
H(14)	-53(5)	-266(6)	734(3)	28(7)
H(15)	-7(4)	-458(5)	783(3)	11(7)
H(16)	6(4)	-517(6)	893(3)	24(8)
H(17)	-43(4)	-356(6)	963(3)	22(7)
H(18)	-89(4)	-170(5)	917(3)	3(7)
H(19)	-93(5)	313(6)	666(3)	37(7)
H(20)	-152(4)	275(5)	598(3)	23(7)
H(21)	-188(4)	223(5)	665(3)	19(7)
H(22)	95(6)	112(7)	589(4)	43(6)
H(23)	9(6)	197(7)	549(4)	49(7)
H(24)	95(6)	250(7)	618(3)	42(7)
H(25)	-234(4)	84(5)	539(3)	7(7)
H(26)	-325(5)	-80(6)	486(3)	34(7)
H(27)	-246(4)	-277(5)	501(3)	18(7)
H(28)	-90(5)	-306(7)	573(3)	41(8)
H(29)	-5(5)	-135(5)	630(3)	19(7)
H(30)	-91(4)	-312(5)	572(3)	24(6)
H(31)	-5(4)	-136(5)	628(2)	0(7)

[a] Fractional coordinates are $\times 10^4$ for non-hydrogen atoms and $\times 10^3$ for hydrogen atoms. B_{iso} values are $\times 10$. [b] Isotropic values for those atoms refined anisotropically are calculated using the formula given by Hamilton, W. C. *Acta Crystallogr.* **1959**, *12*, 609.

expects the spectrum to be neither a doublet nor a 1:2:1 triplet, but something in between, and presumably more like a doublet because the angle is closer to 90° than 180°. The observed spectrum fits this description, and in fact this type of spectrum has been observed before in (1-R-3,4-dimethylphosphole)$_2$Ru(CO)$_2$Cl$_2$ systems.[22]

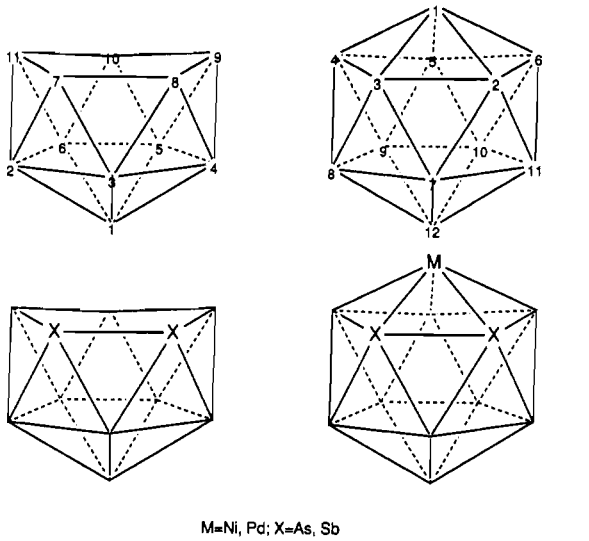

Figure 1. Geometry and numbering systems for $B_9H_{10}X_2^-$ (left), and icosahedral metallaheteroboranes (right).

Mass Spectroscopy. A low resolution electron impact mass spectrometric analysis was attempted on $(PMe_2Ph)_2Pd(B_9H_9As_2)$. The calculated molecular weight for $C_{16}H_{31}As_2B_9P_2Pd$ is 638.90, however, no parent ion was observed. The principal fragment clusters are centered at m/e = 563, 530, 389, and 319; the spectrum cuts off at m/e = 565. The fragment centered at m/e = 563 corresponds to loss of a Ph from the parent ion.

Visible Spectra. The visible spectra of the M = Ni, Pd, and Pt[23] analogues of $(PMe_2Ph)_2M(B_9H_9As_2)$ indicate different λ_{max}, as expected from their different colors, green, purple, and orange, respectively. We believe the colors to arise primarily from d–d electronic transitions, which is supported by the magnitude of the molar absorptivity coefficients, about 10^2 cm^{-1} M^{-1}. Furthermore, the differences in λ_{max} arise from differences in the magnitude of the d–d splitting energies; i.e., the heaviest analogue, Pt, is expected to have the greatest d–d splitting energy,[24] so it absorbs at the lowest λ_{max}, 482 nm. Conversely, the lightest analogue, Ni, is expected to have the smallest d–d splitting energy, so it absorbs at the highest λ_{max}, 624 nm. The Pd analogue falls in between, with λ_{max} = 538 nm.

Derivatives with a Phosphine Bonded to Boron. In the reaction of $(PMe_2Ph)_2NiCl_2$ with $B_9H_9As_2^{2-}$, one other compound in addition to $(PMe_2Ph)_2Ni(B_9H_9As_2)$ was formed in low yield. This second compound (**2**) is believed to be formed by a phosphine–hydride interchange to give $(PMe_2Ph)HNi(5\text{-}PMe_2Ph\text{-}B_9H_8As_2)$ which then undergoes hydrogen–chlorine exchange to generate **2**. This type of phosphine–hydride interchange reaction has been reported for a number of (phosphine)metallacarborane complexes containing nickel,[8,9] platinum,[25] rhodium,[26] and ruthenium.[27,28] The metal–hydride products were not isolated but reacted with chlorinating agents[29] to form the chlorometal compounds described above.

Compound **2** exhibits a 1:2:2:1:3 peak area ratio in the $^{11}B\{^1H\}$ NMR spectrum, which is consistent with C_s symmetry. One of

(21) Jenkins, J. M.; Shaw, B. L. *J. Chem. Soc. A* **1966**, 770.

(22) Wilkes, L. M.; Nelson, J. H.; McCusker, L. B.; Seff, K.; Mathey, F. *Inorg. Chem.* **1983**, *22*, 2476.

(23) Jasper, S. A., Jr. Unpublished data, Indiana University, 1991.

(24) Greenwood, N. N.; Earnshaw, A. *Chemistry of the Elements*; Pergamon Press: Oxford, 1984; p 1096.

(25) Barker, G. K.; Green, M.; Stone, F. G. A.; Welch, A. J.; Wolsey, W. C. *J. Chem. Soc., Chem. Commun.* **1980**, 627.

(26) Baker, R. T.; Delaney, M. S.; King, R. E., III; Knobler, C. B.; Long, J. A.; Marder, T. B.; Paxson, T. E.; Teller, R. G.; Hawthorne, M. F. *J. Am. Chem. Soc.* **1984**, *106*, 2965.

(27) Jung, C. W.; Hawthorne, M. F. *J. Am. Chem. Soc.* **1980**, *102*, 3024.

(28) Jung, C. W.; Baker, R. T.; Hawthorne, M. F. *J. Am. Chem. Soc.* **1981**, *103*, 810.

(29) Collman, J. P.; Hegedus, L. S. *Principles and Applications of Organotransition Metal Chemistry*; University Science Books: Mill Valley, CA, 1980.

the area 1 signals is a doublet in the proton-decoupled ^{11}B NMR spectrum, which indicates that there is a B–P bond. Furthermore, the phosphine attached to the cage must be located on the plane of symmetry in order to maintain the C_s symmetry of the molecule. There are three unique boron atoms for the phosphine to be attached to, B(5), B(7), and B(12). The X-ray structure of the Pd derivative **3** demonstrates that the phosphine is attached to the B(5) cage atom. Therefore it is assumed that the phosphine is on B(5) in **2** as well. The $^{31}P\{^1H\}$ NMR contains a 1:1:1:1 quartet, which is consistent with the existence of a B–P bond; in addition, there is also a singlet due to the phosphine on nickel. The J_{B-P} value of 130 Hz for **2** is at the lower end of the range (128–145 Hz) observed previously for similar derivatives.[9,27]

The ^1H NMR of **2** contains two doublets in the methyl region of the spectrum, which suggests that the two methyl groups on each phosphine are chemically equivalent on the NMR time scale at 21°. This in turn suggests that there is rapid rotation about the pseudo-five-fold axis through nickel and the B_3As_2 face; otherwise, the methyls on each phosphine would experience different chemical environments. This type of rotation is quite common in metallaboranes, and variable temperature proton NMR studies have been used to determine the energy of activation associated with this rotational process.[30] These studies have not yet been attempted for the molecules under consideration here, however, there is an area for future study. The different environment of each pair of methyl protons is manifested both by the different chemical shift of each pair and by the different H–P coupling constants.

Hawthorne et al.[9] have proposed an intramolecular phosphine–hydride interchange mechanism for the isoelectronic $(PPh_3)_2Ni[B_9H_9(CH)_2]$ system. Attempts to duplicate phosphine–hydride interchange on the arsaborane systems under the same conditions (refluxing benzene) failed. Also, refluxing with benzene, THF, or monoglyme in the presence of tBuCl failed to produce substantial quantities of phosphine–hydride interchanged products.

However, the inclusion of $(PMe_2Ph)_2MCl_2$ (M = Ni or Pd) in THF solution allows phosphine–hydride interchange to occur in $(PMe_2Ph)_2M(B_9H_9As_2)$ species at room temperature. We therefore suggest that in our system there may be an intermolecular process operating, which involves the metal center of a reactive intermediate derived from $(PMe_2Ph)_2MCl_2$. Interestingly, this isomerization was not observed to occur in CH_2Cl_2, but it would occur in THF. This suggests that the rearrangement reaction may be assisted by Lewis bases. Further studies of this process are in progress.

During flash column chromatography of the reaction mixture that contained $(PMe_2Ph)_2Pd(B_9H_9As_2)$, two green bands, $(PMe_2Ph)ClPd(6\text{-}Cl\text{-}5\text{-}PMe_2Ph\text{-}B_9H_7As_2)$ (compound **4**) and the previously reported[6] $(PMe_2Ph)ClPd(5\text{-}PMe_2Ph\text{-}B_9H_8As_2)$, were collected. Both of these compounds are formed by some phosphine–hydride interchange process. In the case of **4**, there is a second metal assisted chloride–hydride interchange as well.

Compound **4**, the first green band to elute during chromatography, has a very distinctive ^{11}B NMR spectrum that requires all nine boron atoms to be chemically inequivalent. The molecule thus has C_1 symmetry. As observed with the other compounds with B–P bonds, one of the $^{11}B\{^1H\}$ peaks of **4** is a doublet due to ^{31}P coupling. The $^{31}P\{^1H\}$ NMR spectrum corroborates this, as there is a 1:1:1:1 quartet and a singlet in the spectrum. The B–P coupling constant, 137 Hz, is within the range of similar previously reported derivatives.[9,27]

The factors influencing the distribution of $(PMe_2Ph)_2Pd(B_9H_9As_2)$ versus the rearranged products, $(PMe_2Ph)ClPd(5\text{-}PMe_2Ph\text{-}B_9H_8As_2)$ or **4**, have not been fully investigated; however, some general conclusions seem evident. In the room temperature

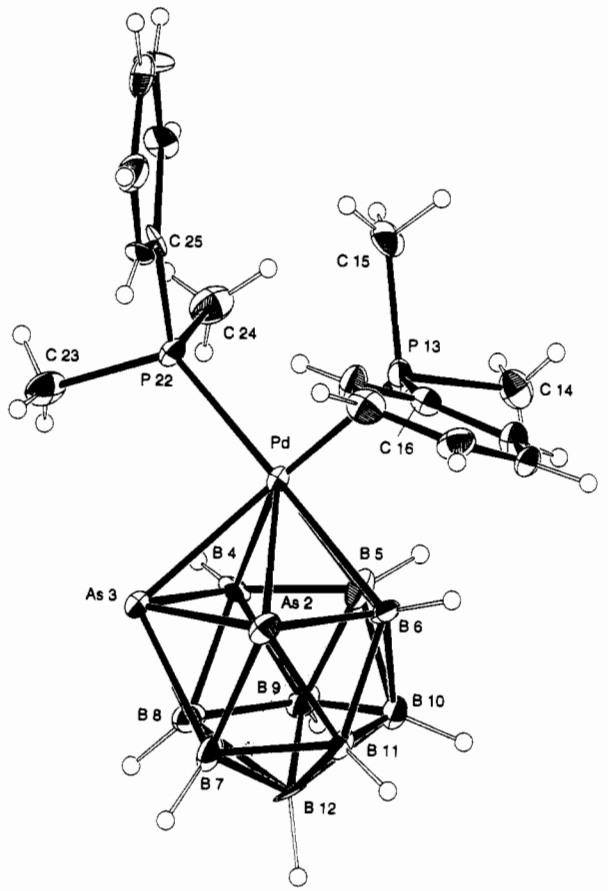

Figure 2. ORTEP diagram of 1,1-$(PMe_2Ph)_2$-*closo*-1,2,3-$PdAs_2B_9H_9$ (**3**).

synthesis of the platinum analogue, no rearrangement product such as $(PMe_2Ph)ClPt(PMe_2Ph\text{-}B_9H_8As_2)$ was observed, although attempts to synthesize this by several methods are in progress. For the palladium case, there is a distribution of $(PMe_2Ph)_2Pd(B_9H_9As_2)$ and $[(PMe_2Ph)ClPd(5\text{-}PMe_2Ph\text{-}B_9H_8As_2)]$ or **4** which favors $(PMe_2Ph)_2Pd(B_9H_9As_2)$ at room temperature.

In an effort to expand the chemistry observed in metallaarsaboranes, the antimony analogue, $(PMe_2Ph)_2Pd(B_9H_9Sb_2)$ (**5**), was synthesized. The $^{11}B\{^1H\}$ NMR spectrum of **5** has peaks with area ratios 1:1:2:2:3, which is consistent with the 2:2:2:1:1:1 pattern expected for a molecule with C_s symmetry. Although the order of the peaks is not quite the same, this spectrum is actually quite similar to that of $(PMe_2Ph)_2Pd(B_9H_9As_2)$, if one allows for slight shifting of this order. A 2D ^{11}B–^{11}B COSY NMR study may confirm this, if the overlapping peaks do not prevent determination of the correlations. The $^{31}P\{^1H\}$ NMR spectrum is simply a singlet, as expected for the two equivalent phosphines.

Structural Considerations. The most striking structural feature of the $(PMe_2Ph)_2Pd(B_9H_9As_2)$ (**3**) and $(PMe_2Ph)_2Pd(B_9H_9Sb_2)$ (**5**) molecules (see Figures 2 and 4) is the distortion of the 12-membered cage that results from the inclusion of the relatively large As, Sb, and Pd atoms. As may be expected, the 2.7996-Å Sb(2)–Sb(3) distance in **5** (see Table VII) is much greater than the typical 1.61-Å C–C distance in the isoelectronic $B_9H_9(CH)_2M$ cage,[31] and even greater than the 2.488-Å As–As distance in **3**. Since these cages are isoelectronic, the cage distortion due to the arsenic and antimony atoms is primarily a steric effect, and not an electronic one. In both **3** and **5**, the bonding of the Pd atom is off of the pseudo-five-fold rotational axis of symmetry; as seen

(30) Marder, T. B.; Baker, R. T.; Long, J. A.; Doi, J. A.; Hawthorne, M. F. *J. Am. Chem. Soc.* **1981**, *103*, 2988.

(31) Fontaine, X. L. R.; Greenwood, N. N.; Kennedy, J. D.; Nestor, K.; Thornton-Pett, M. *J. Chem. Soc., Dalton Trans.* **1990**, 681.

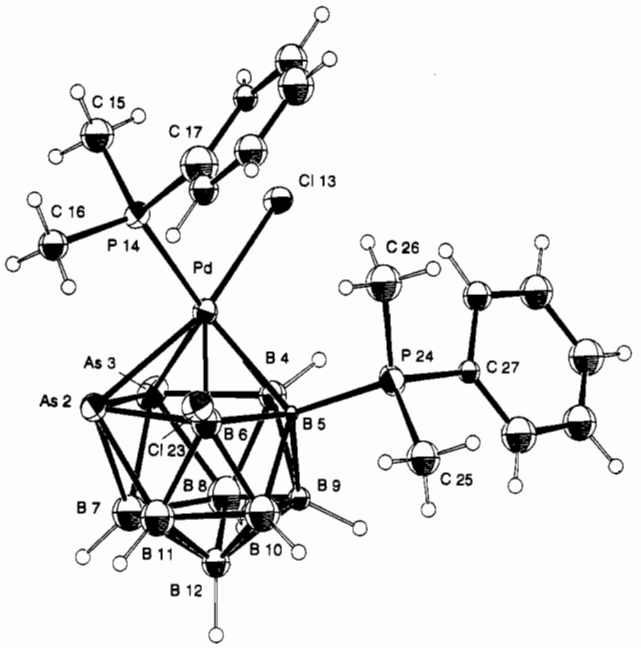

Figure 3. ORTEP diagram of 1,6-Cl_2-1,5-$(PMe_2Ph)_2$-*closo*-1,2,3-$PdAs_2B_9H_7 \cdot CH_2Cl_2$ (**4**).

by the bonding distances Pd–As(2) = 2.6835(18) Å, Pd–As(3) = 2.5304(13) Å, Pd–B(4) = 2.298(11) Å, Pd–B(5) = 2.283(12) Å, and Pd–B(6) = 2.309(10) Å for **3** and Pd–Sb(2) = 2.7865 Å, Pd–Sb(3) = 2.7074 Å, Pd–B(4) = 2.290 Å, Pd–B(5) = 2.304 Å, and Pd–B(6) = 2.290 Å for **5**, the Pd is farthest from the two As or Sb atoms.

The inclusion of three large heteroatoms in a single triangular face of an icosahedron causes the cage to "flex" outward to accommodate the larger atoms. This effect is illustrated by contrasting intraboron distances between boron atoms adjacent to a heteroatom and boron atoms not adjacent to a heteroatom. For example, in **3**, the average B–B distance in the chair-shaped trace defined by atoms 4–5–6–11–7–8 (see Figure 5) is 1.845 Å; in **5**, the corresponding average B–B distance is 1.844 Å. However, in the isoelectronic carborane *closo*-1,1-$(PR_3)_2$-1,2,3-$PtC_2B_9H_{11}$,[32] the corresponding average B–B distance is 1.799 Å; in $Ni(C_2B_9H_{11})_2$,[33] it is 1.800 Å. In all of the above cages, the average B–B distance in the triangle opposite the three heteroatoms, atoms 9–10–12, is 1.76–1.77 Å. This agrees with the value for $B_{12}H_{12}^{2-}$,[34] 1.77 Å.

The X-ray structures of these species indicate that the P–M–P plane is essentially parallel to the X–X vector, and this has been explained in frontier molecular orbital terms for the $[(PH_3)_2Pt]$ and $[B_9H_9(CH)_2]$ fragments.[32] The principal bonding interaction involves the HOMO of $[(PH_3)_2Pt]$, which is a hybrid MO with large Pt d_{xz} character and either the LUMO or second LUMO (SLUMO), which is close in energy, of $[B_9H_9(CH)_2]$; see Figure 6. The LUMO contains a plane of symmetry that bisects the X–X vector, and a HOMO–LUMO interaction favors the P–M–P plane being perpendicular to the X–X vector; the SLUMO has a node at the symmetrically unique B on the B_3X_2 face, and a HOMO–SLUMO interaction favors the P–M–P plane being parallel to the X–X vector. Both conformations are apparently similar in energy, and in fact cocrystallization of the two conformations, resulting in a disordered X-ray crystal structure of $(PPh_3)_2Pt(B_9H_9As_2)$, has recently been observed.[6]

The X-ray crystal structures of **3** and **5** show that the Pd–As and Pd–Sb distances are not equal: Pd–As(2) is 2.6835(13) Å and Pd–As(3) is 2.5304(13) Å; similarly, Pd–Sb(2) is 2.7074 Å and Pd–Sb(3) is 2.7865 Å. Also, the P–Pd–P plane is nearly, but not exactly, parallel to the X–X vector. There is significant twisting of the $(R_3P)_2Pd^{2+}$ fragment relative to the B_3X_2 face such that one R_3P is closer to the X atoms than the other. This asymmetry is consistently observed in crystal structures of the type $(R_3P)_2M(B_9H_9X_2)$ (M = Pd, Pt; X = CH, As, Sb). This means that the $[(R_3P)_2Pd]$ HOMO is twisting such that one lobe is closer to, and thus has better overlap with, the same X atom.

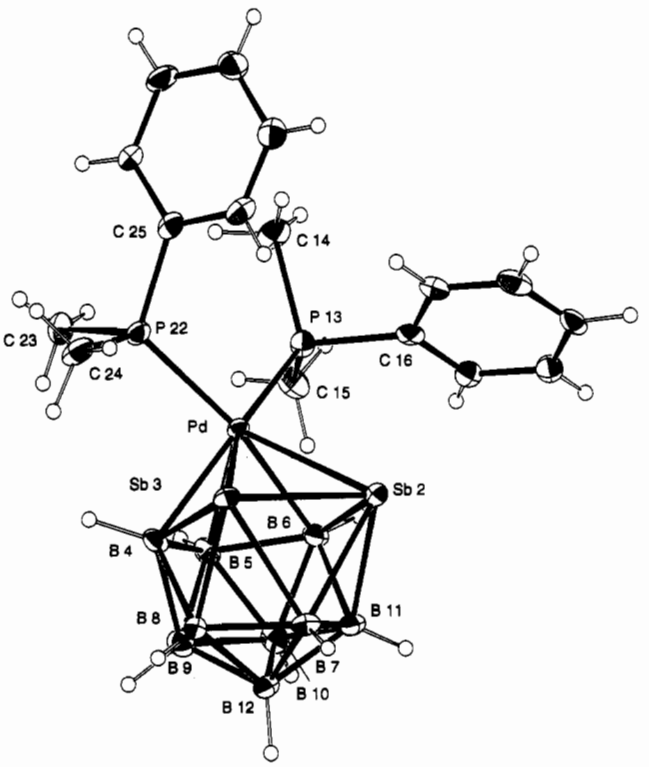

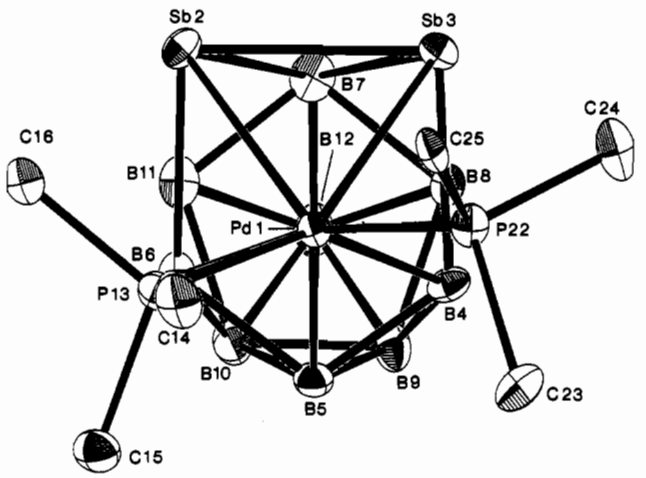

Figure 4. (a) ORTEP diagram of 1,1-$(PMe_2Ph)_2$-*closo*-1,2,3-$PdSb_2B_9H_9$ (**5**). (b) ORTEP diagram showing view along Pd(1)–B(12) axis of 1,1-$(PMe_2Ph)_2$-*closo*-1,2,3-$PdSb_2B_9H_9$ (**5**).

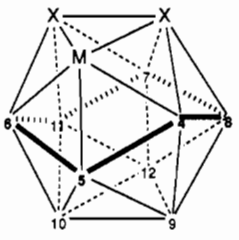

Figure 5. Icosahedral metallaheteroborane indicating long B–B distances along chair-shaped trace (thick lines).

(32) Mingos, D. M. P.; Forsyth, M. I.; Welch, A. J. *J. Chem. Soc., Dalton Trans.* **1978**, 1363.
(33) St. Clair, D.; Zalkin, A.; Templeton, D. H. *J. Am. Chem. Soc.* **1970**, *92*, 1173.
(34) Lipscomb, W. N. *Boron Hydrides*; W. A. Benjamin, Inc.: New York, 1963; p 18.

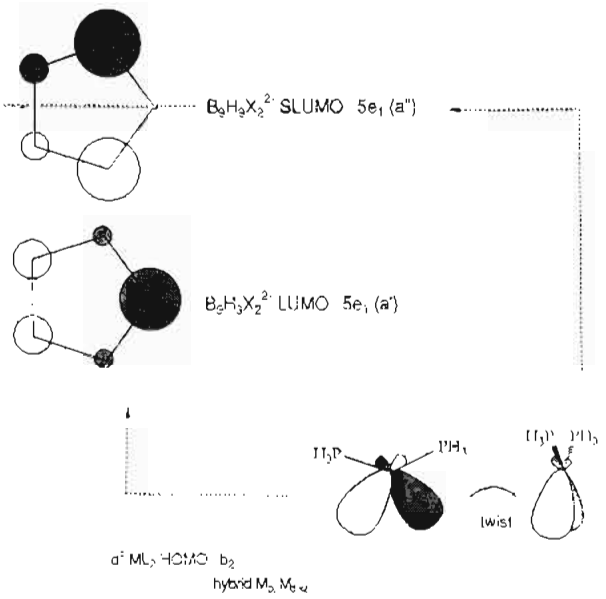

Figure 6. Frontier highest occupied molecular orbital (HOMO), lowest unoccupied molecular orbital (LUMO), and second lowest unoccupied molecular orbital (SLUMO) of $[(PH_3)_2Pt]$ and $[B_9H_9(CH)_2]$ fragments.

Thus, there are two different Pd–X distances, and the shorter is always on the side where the R_3P is closer to the X atoms. The twisting of the $(R_3P)_2M^{2+}$ fragment may be due to crystal packing forces, as all of the aforementioned crystals have the same space group.

Of the three As–B or Sb–B distances for each heteroatom, one is short and two are long. The long bonds involve the B atoms that are bonded to two heteroatoms (Pd, As, or Sb) rather than just one. This observation is in accord with structural details of other metallaheteroboranes.[35,36,37]

A single-crystal X-ray diffraction study of 1,6-Cl_2-1,5-$(PMe_2Ph)_2$-1,2,3-$PdAs_2B_9H_7$-CH_2Cl_2 (**4**) was undertaken to firmly establish which structural isomer it is, and to more closely examine structural data; see Figure 3. As in the parent molecule **3**, the B_9PdAs_2 cage is significantly distorted from a regular icosahedron, due primarily to the large arsenic and palladium atoms in the cage. As can be seen in Tables I and IV, the bond lengths associated with the B_9PdAs_2 cages of these complexes are not greatly changed. The most significant changes are lengthening of the B(4)–B(5) distance from 1.755(16) to 1.85(5) Å and the As(2)–B(6) distance from 2.184(11) to 2.26(4) Å, along with concomitant shortening of the B(5)–B(6) distance from 1.881(17) to 1.73(5) Å. The B(5)–P(24) distance of 1.95(3) Å is similar to the B–P distances in other phosphine–hydride exchanged metallaheteroboranes in the range 1.92–1.948(8) Å.[6,9,25]

The B(6)–Cl(23) distance of 1.81(4) Å is similar to the B–Cl distances in some other metallaborane compounds, 7-(C_5Me_5)-*nido*-7,12-$RhOB_{10}H_9$-8-Cl-11-PMe_2Ph,[38] 1.823(6) Å; 7-(C_5Me_5)-*nido*-7-$RhB_{10}H_{11}$-8-Cl-11-PMe_2Ph-CH_2Cl_2,[38] 1.862(7) Å; 8-Cl-7,9-$(PPh_3)_2$-7-(*o*-$Ph_2PC_6H_4$)-*isonido*-7-IrB_9H_6-10,[39] 1.916(26) Å; and 3-Cl-7,9-$(PPh_3)_2$-7-(*o*-$Ph_2PC_6H_4$)-*isonido*-7-IrB_9H_8-10,[39] 1.790(16) Å; and some boron subhalides, B_8Cl_8 and B_9Cl_9,[40] 1.74 Å.

Acknowledgment. We thank professor Odile Eisenstein for helpful discussions.

Supplementary Material Available: Tables of anisotropic thermal parameters, bond distances, and intramolecular angles (31 pages). Ordering information is given on any current masthead page.

(35) Ferguson, G.; Kennedy, J. D.; Fontaine, X. L. R.; Faridoon; Spalding, T. R. *J. Chem. Soc., Dalton Trans.* **1988**, 2555.
(36) Faridoon; Ni Dhubhghaill, O.; Spalding, T. R.; Ferguson, G.; Kaitner, B.; Fontaine, X. L. R.; Kennedy, J. D.; Reed, D. *J. Chem. Soc., Dalton Trans.* **1988**, 2739.
(37) Faridoon; Ni Dhubhghaill, O.; Spalding, T. R.; Ferguson, G.; Kaitner, B.; Fontaine, X. L. R.; Kennedy, J. D. *J. Chem. Soc., Dalton Trans.* **1989**, 1657.
(38) Fontaine, X. L. R.; Fowkes, H.; Greenwood, N. N.; Kennedy, J. D.; Thornton-Pett, M. *J. Chem. Soc., Dalton Trans.* **1987**, 2417.
(39) Bould, J.; Kennedy, J. D.; Thornton-Pett, M. *J. Chem. Soc., Dalton Trans.* **1992**, 563.
(40) Greenwood, N. N.; Earnshaw, A. *Chemistry of the Elements*; Pergamon Press: Oxford, 1984; p 228.